

1 **Hydrological processes and permafrost regulate magnitude, source**
2 **and chemical characteristics of dissolved organic carbon export in a**
3 **peatland catchment of northeastern China**

4

5 Yuedong Guo¹, Changchun Song¹, Wenwen Tan¹, Xianwei Wang¹, Yongzheng Lu¹

6 ¹Key Laboratory of Wetland Ecology and Environment, Northeast Institute of
7 Geography and Agroecology, Chinese Academy of Sciences, Changchun 130102,
8 China

9 *Correspondence to:* Changchun Song (songcc@iga.ac.cn)

10

11 **Abstract.**

12 Permafrost thawing in peatlands has the potential to alter the catchment export of
13 dissolved organic carbon (DOC), thus influencing the carbon balance and cycling in
14 linked aquatic and ocean ecosystems. Peatlands along the southern margins of the
15 Eurasian permafrost are relatively understudied despite the considerable risks
16 associated with permafrost degradation due to climate warming. This study examined
17 dynamics of DOC export from a permafrost peatland catchment located in
18 northeastern China during the 2012 to 2014 growing seasons. The estimated annual
19 DOC loads varied greatly between 3211 to 19022 kg yr⁻¹ with a mean DOC yield of
20 4.7 g m⁻² yr⁻¹. Although the estimated DOC yield was in the lower range compared
21 with other permafrost regions, it was still significant for the net carbon balance in the
22 studied catchment. There were strong linkages between daily discharge and DOC
23 concentrations in both wet and dry years, suggesting a transport-limited process of
24 DOC delivery from the catchment. Discharge explained the majority of both seasonal
25 and inter-annual variations of DOC concentrations, which made annual discharge a
26 good indicator of total DOC load from the catchment. As indicated by three

27 fluorescence indices, DOC source and chemical characteristics tracked the shift of
28 flowpaths during runoff processes closely. Interactions between the flowpath and
29 DOC chemical characteristics were greatly influenced by the seasonal thawing of the
30 soil active layer. The deepening of the active layer due to climate warming likely
31 increases the proportion of microbial-originated DOC in baseflow discharge.

32

33 **1 Introduction**

34 Permafrost soils have acted as sinks for atmospheric carbon (C) since at least the
35 late Pleistocene and serve as key sources of dissolved organic carbon (DOC) for
36 linked aquatic and ocean ecosystems (Opsahl et al., 1999; Kicklighter et al., 2013).
37 Because changes in the quantity and quality of exported DOC can greatly alter the
38 energy cycles of the linked oceans, considerable progress has been made in recent
39 years to better evaluate potential changes in DOC export patterns from permafrost
40 regions (Townsend-Small et al., 2011; Vonk et al., 2013). However, uncertainties
41 remain regarding the primary drivers and the fate of DOC due to complex interactions
42 between hydrological and thermal dynamics as well as bio-chemical drivers (Olefeldt
43 and Roulet, 2012; Kicklighter et al., 2013).

44 Significant losses of near-surface permafrost have been observed over the past
45 century and such outcomes have induced considerable changes in hydrological
46 processes and soil thermal regimes (Lyon et al., 2009; Lessels et al., 2015), in turn
47 altering the magnitude and timing of terrestrial DOC export processes. Flow pathway
48 is an important and well-documented regulator of DOC export from permafrost
49 regions (Ågren et al., 2010; Guo et al., 2015). Owing to increased levels of
50 hydrological access to previously frozen soils following permafrost degradation, DOC
51 export was forecast to increase in Siberian rivers along a latitudinal transect (Frey and
52 MacClelland, 2009). However, permafrost degradation also increased the likelihood
53 of interactions between subsurface flows and mineral soils, which should lead to
54 considerable DOC absorption by fine soil particles and in turn decrease in DOC

55 export magnitude (Petronne et al., 2006; Striegl et al., 2005). There were significant
56 disparities in DOC export concentrations and seasonal patterns between surface- and
57 subsurface-dominated runoff processes in permafrost catchments (Laudon et al.,
58 2011). The capacity for DOC export from permafrost soils was closely linked to
59 lateral subsurface flow (Striegl et al., 2007; Lyon et al., 2010). Therefore, alterations
60 to flow pathways during permafrost freeze-thaw cycles are some of the most
61 important factors to consider in evaluating DOC export potential in a peatland.

62 Flow pathways also determine chemical composition of the DOC exported from
63 permafrost catchments, which in turn can influence downstream DOC mineralization
64 rates and carbon emissions from streams, lakes and oceans (Mann et al., 2012; Cory et
65 al., 2014). DOC composition can be by flow pathways along the organic-mineral soil
66 layer. Mineral soil particles preferentially absorbed dissolved organic matter high in
67 aromatic components with large molecular weights or acidic functional groups, and
68 aromatic structures (Kalbitz et al., 2005). In contrast, hydrophilic fatty microbial
69 products with low molecular weights were desorbed and released (Striegl et al., 2005).
70 To date, a partial theoretical framework and methods have been developed to
71 understand alterations in DOC chemical characteristics following permafrost
72 degradation (Spencer et al., 2015). But uncertainties still exist in understanding the
73 entire way hydrological processes affect the magnitude and chemical characteristics
74 of DOC exported from permafrost peatland catchments.

75 Given the high spatial heterogeneity of peatlands and the complexity of
76 hydrological processes in permafrost regions, it is important to understand the
77 magnitude and controls on DOC export in different permafrost regions, especially in
78 the south part of the Eurasian continent where limited research has been performed to
79 date. Our study focused on dynamics of DOC release from the Fukuqi River, a
80 tributary of the Amur River positioned along the northern slopes of the Great Xing'an
81 Mountains in northeastern China. The Great Xing'an Mountains form an important
82 barrier from Siberian cold air masses and monsoons of East Asia. The mean annual
83 temperature of the area has on average increased by 0.3 °C every 10 years over the

84 last 50 years, and the thickness of the active layer has increased by 20-40 cm on the
85 southern slopes of the Great Xing'an Mountains from the 1970s to 2000 (Jin et al.,
86 2000). However, few studies have focused on possible consequences of permafrost
87 degradation in this region to date. This work thus investigated potential changes in
88 DOC export patterns by answering the following questions:

89 (1) What is the DOC load transported by discharge from the entire catchment?

90 (2) What is the relationship between runoff processes and concentrations, sources,
91 and chemical characteristics of DOC?

92 **2 Approach and methodology**

93 **2.1 Study area**

94 Northern sections of the Great Xing'an Mountains in China are located along the
95 southern margins of the continuous permafrost zone in Eurasia. The area represents
96 the most remote region of the East Asia monsoon of the East Eurasian continent. The
97 region includes approximately 8.245×10^3 km² of natural wetlands, representing a
98 major proportion of cold temperate wetlands and an important reservoir of soil carbon
99 and usable water resources for northeastern China.

100 The Fukuqi River, a second order branch of the Amur River, is located in the
101 continuous permafrost of the northern slope of the Great Xing'an Mountains (Fig. 1).
102 The catchment extends across an area of 287 km² with an annual mean temperature of
103 -4.2 °C and a mean annual precipitation of 425 mm (1959-2013). Peatland covers the
104 flat river valley and ranges in altitude from 500 to 580 m. Mountains surround the
105 peatland and have a much steeper slope than the peatland (Fig. 1). The peat layer,
106 which is approximately 0.3-0.4 m thick, is composed of typical organic soil with
107 organic matter levels ranging from 40% to 60% and with porosity levels ranging from
108 60% to 20% near the surface. According to previous field surveys, the peatlands
109 accounts for more than 90% of the total carbon stock in the catchment but covers only
110 about one-third of the total area. The maximum thaw depth of the active layer,
111 ranging from 60 to 80 cm, occurs usually in early August. Below the peat soil layer is

112 mineral soil with a much lower organic content (< 5%) and soil porosity (< 10%) than
113 the upperpeat soil. Sphagnum mosses (*S. capillifolium*, *S. magellanicum*) and sedges
114 (*Eriophorum vaginatum*) are the dominant vegetation. The growing season is from
115 May until late September. The upland mountains on both sides of the valley are
116 extensively covered by mineral soil and gravels with little organic content due to the
117 continuous logging and frequent fires during the past 60 years. The original
118 coniferous forest has been replaced by planted young *Pinus sylvestris var. mongolica*.
119 The maximum thaw depth of the forest ranges from 80 to 100 cm, which is slightly
120 deeper than the peatland.

121

122 **Figure 1**

123

124 **2.2 Sampling and monitoring program**

125 Monitoring was conducted from early May to late September in 2012, 2013 and
126 2014. A gauging station to profile DOC concentrations and hydrological parameters
127 was set for the lower reaches of the Fukuqi River (Fig. 1). Water samples were
128 collected from the stream profile every 1–5 days with 200 ml polyethylene bottles. A
129 higher sampling frequency was applied during flood events whereas a lower sampling
130 frequency was using during periods of low water. Soil pore water in the peatland was
131 collected from three sites located 50-100 m away from the main river channel on the
132 8th June, 30th June, 27th July and 25th August in 2013 (Fig. 1). When sampling, 100 ml
133 samples of soil pore water were collected at 10 cm intervals along the active layer
134 using ceramic soil pore water samplers (SIC20, Germany). Porewater was collected
135 from the same 3-5 locations at each of the three sites for each sampling period. Due to
136 the gradual thawing of the active layer during the growing seasons, the maximum
137 sampling depths differed for each of the four sampling periods. The water samples
138 were filtered through a 0.45-µm glass fibre membrane, and stored in 4°C in the dark
139 for at most seven days before analysis using a DOC analyser (C-VCPH, Shimadzu,

140 Japan) (Guo et al., 2014). The river began to freeze after September in each year, and
141 flow under the ice was not detected during the winter.

142 Discharge (Q) from through the gauging profile was calculated by measuring
143 water level and flow velocity automatically using a water level monitor (Odyssey,
144 New Zealand, accuracy: ± 2 mm) and a flow meter (Argonaut-ADV, USA, accuracy:
145 ± 0.01 m s⁻¹). Air temperature and soil temperature at 0–1.0 m depth were also
146 recorded by an automatic microclimate gauging tower (CS3000, Campbell, USA) set
147 in the center part of the peatlands. Water level in the peatland was recorded
148 continuously near the gauging tower with the same Odyssey monitor. The thaw depth
149 of the peatland active layer was manually surveyed weekly with a 1.0-m stainless
150 steel ruler (accuracy: 0.1 cm) at the same three sites. Information of the temperature
151 ($^{\circ}$ C), electrical conductivity (mS cm⁻¹), and turbidity (NTU) in the sampling profile
152 was logged continuously using a multi-parameter water quality sonde (6600EDS, YSI,
153 USA). About one-fifth of the water quality data mainly in May and late September
154 were lost because of equipment malfunction at low temperature. All the instruments
155 were set to collect data every six hours while they were being deployed while they
156 were being deployed.

157 **2.3 Fluorescence measurements**

158 Excitation-emission matrixes (EEMs) of the water samples were measured using
159 a Hitachi F-7000 fluorescence spectrometer (Hitachi High Technologies, Japan) with
160 a 50 W ozone-free Xenon arc lamp and R928P photomultiplier tube fitted as a
161 detector. The spectrometer was set to collect signals using a 5-nm bandpass on
162 excitation and emission monochromators at a scanning speed of 3,200 nm min⁻¹. EEMs
163 were recorded for excitation spectra of between 220 and 400 nm and for emission
164 spectra of between 300 and 500 nm. To eliminate the inner-filter effect, samples were
165 diluted with deionized water to a UV absorbance at $\lambda = 254$ nm of 0.2 absorbance
166 units (cm⁻¹). Milli-Q water blank EEMs were subtracted from the sample EEMs to
167 eliminated Raman scatter peaks. Then, the EEMs were normalized to the area under
168 the Raman scatter peak (excitation wavelength of 350 nm) of a Milli-Q water sample

169 run the same day. The fluorescence intensities measured were reported in Raman
170 Units (RU) in this study.

171 Three spectral indices were calculated from the EEMs to quantify chemical
172 characteristics of the dissolved organic matter. The humification index (HIX) is
173 defined as the ratio of the sum of $\lambda_{em} = 435\text{--}480$ nm to the sum of $\lambda_{em} = 300\text{--}345$ nm
174 excitation at 254 nm and quantifies the complexity and aromaticity of dissolved
175 organic matter. High HIX values denote the presence of highly humified or more
176 complex organic matter (Ohno, 2002). The fluorescence (FI) was the second index
177 and is defined as the ratio of fluorescence emission intensities at 470 and 520 nm for
178 excitation at 370 nm. The recommended FI for plant-derived organic matter is 1.3-1.4
179 and that for materials of microbial origin is 1.7-2.0 (McKnight et al., 2001). The third
180 index we measured was the biological index (BIX), defined as the ratio of
181 intensities at λ_{em} 380 nm and 430 nm for excitation at 310 nm. BIX ranges from 0.6 to
182 1.0 or greater generally, and is a complementary index for evaluating the relative
183 contributions of microbial-derived organic matter (Huguet et al., 2009). Lower values
184 mean proportionately less microbial-derived organic matter.

185 **2.4 Estimation of DOC load and yield**

186 A web-based program LOADEST was used to estimate the DOC load for the three
187 years (<https://engineering.purdue.edu/mapserve/LOADEST/>). LOADEST uses linear
188 regression models to identify relationships between discharge and DOC
189 concentrations, and in turn to estimate daily DOC load by applying the statistical
190 method of Adjusted Maximum Likelihood Estimation (AMLE), Maximum Likelihood
191 Estimation (MLE), and least absolute deviation (LAD). In total, eleven models are
192 used in the program, and the best one was automatically selected to fit the data on the
193 base of Akaike Information Criterion (Park et al., 2015). In our study, 36, 35, and 31
194 measurements were used to calculate DOC loads for the years 2012, 2013, and 2014
195 respectively. Loads were estimated using the MLE method according to the standard
196 error (SE) and the distribution of the residuals. The DOC yield was calculated as the
197 load divided by the entire catchment area.

198 **2.5 Statistical analyses**

199 The mean and the standard deviation of the DOC concentrations in the stream and
200 soil pore water, and the three fluorescence indices were statistically analyzed with the
201 Statistical Program for Social Sciences (SPSS) version 13.0 software. The relationship
202 between the hydrological factors and the DOC concentration and the fluorescence
203 indices was examined by a two-tailed Pearson correlation and regression analysis,
204 where the p-values were calculated to test for significance. Analysis of covariance
205 (ANCOVA) was also conducted to distinguish if the relationships between discharge
206 and the DOC characteristics (concentration and fluorescence indices) were
207 statistically different for different years, and if there were other factors controlling the
208 DOC characteristics besides discharge.

209 **3 Results**

210 **3.1 Environmental conditions**

211 Substantial inter-annual and seasonal variations in precipitation were observed for
212 the three years (Fig. 2). The total precipitation reached 202.5, 520.8 and 164 mm in
213 2012, 2013 and 2014, respectively. Based on our statistics on the regional climate
214 dataset from 1970 to 2005, 2013 was an extremely wet year due to excessive rainfall
215 occurring in the spring and summer. The total rainfall in 2012 was within a normal
216 range while that for 2014 indicated an extreme dry year. Probably owing to the
217 abundant rainfall in 2013, the air temperature during the growing season in this year
218 with a mean value of 12.9°C, was lower than those of 2012 and 2014 (on average
219 13.7°C). However, mean values in all three years were within the average long-term
220 range. We also found no significant differences in the maximum thaw depths of soil
221 active layer for the three years. The standing water levels in the peatland close to the
222 stream channel declined gradually across the growing seasons probably due to the
223 deepening of active layer. Water levels in the peatland were always lower than peat
224 surface during the three years of sampling.

225

226 **Figure 2**

227

228 **3.2 DOC concentrations and loads**

229 DOC concentrations in the Fukuqi River fluctuated considerably with stream
230 discharge during the three growing seasons (Fig. 3). The mean DOC concentration in
231 2013 was significantly larger than that in 2012 and 2014 (Table 1). Great seasonal
232 variability was clearly observed for all of the three years, which mainly resulted from
233 the varied rainfall patterns as shown in Fig. 2. In the three years of measurements, the
234 maximum concentration of 44.7 mg L⁻¹ was found in the early spring of 2013 and was
235 accompanied by the peak flood occurring during the three years. The estimated DOC
236 loads and yields for the three years varied greatly (Table 1). The total load, as well as
237 the DOC yield in the wet year of 2013 was about six times that of the extreme dry
238 year of 2014. The annual load and yield in 2012 differed greatly compared with 2014,
239 but the estimated mean concentrations were quite similar. Monthly variability in loads
240 was also found, with maximum values occurring either in May or August. The mean
241 DOC load for the three years was 4.7 g m⁻² yr⁻¹. Several large floods contributed the
242 majority of the load. Statistically, nine flood events (maximum discharge > 1.0 × 10⁶
243 m³ d⁻¹) were responsible for 81% of the load while five floods with a discharge level >
244 2.0 × 10⁶ m³ d⁻¹ accounted for 65% of the total load.

245

246 **Figure 3**

247

248 **Table 1**

249

250 Significant positive correlations were found between DOC concentrations and
251 discharge for all three growing seasons (Fig. 4). However, results of covariance
252 analysis suggested that the adjusted mean DOC concentrations after eliminating the

253 influence of discharge were statistically different for the three years. This result
254 suggested an inter-annual variability in the linear relationship between DOC
255 concentration and discharge (Table 2). As indicated by Adj. R^2 , about sixty percentage
256 of the DOC variability could be explained by the discharge, and the percentage was
257 very similar for the three years. However, the mean residuals for the three linear
258 models were quite different. Tables 2 and 3 suggest that the greater mean residuals
259 were accompanied by a wider concentration range. Large concentration fluctuations
260 would lead to a decreased average predictive ability by discharge. DOC
261 concentrations were positively related to turbidity and negatively related to
262 conductivity ($n=68$, $p < 0.01$) while no significant relationship was found between the
263 concentrations and air temperature or the soil temperatures of active layer.

264

265 **Figure 4**

266

267 **Table 2**

268

269 **Table 3**

270

271 **3.3 Fluorescence indices**

272 The three spectral indices varied considerably with discharge during the growing
273 seasons (Fig. 5). There was a significant positive correlation between the HIX and
274 logarithmic discharge but both FI and BIX were negatively correlated with discharge
275 for (Fig. 6). HIX ranged from 5.52 to 16.41 with an average value of 10.38, revealing
276 a high proportion of more humified components in the stream discharge DOC. FI and
277 BIX values ranged from 1.43 to 1.62 and from 0.46 to 0.63 with average values of
278 1.52 and 0.54, respectively. The FI values indicate that DOC originated both from
279 plant-derived organic matter and from microbial-mediated organic matter while the

280 BIX value denotes the presence of a low proportion of young organic matter from
281 biological sources in the discharge (see Huguet et al., 2009). All three indices were
282 closely related to DOC concentrations and hydrological variables during the entire
283 study period. Only HIX also showed a significant relationship with soil temperature
284 (Table 4). In spite of the great variations during the three growing seasons, the mean
285 annual values of the three indices did not differ statistically for the three years
286 according to the covariance analysis, which eliminated the influence of discharge
287 (Table 5).

288

289 **Figure 5**

290

291 **Figure 6**

292

293 **Table 4**

294

295 **Table 5**

296

297 **3.4 Concentrations and fluorescence indices of soil water**

298 During the growing seasons 2013, soil porewater DOC concentrations in the three
299 points presented similar vertical profiles. Maximum DOC concentrations were
300 typically found at the depth of 20-30 cm in the organic soil layer while the minimum
301 values were found at the deeper mineral layer (Fig. 7). The vertical variation in DOC
302 concentrations could be clearly observed when the active layer reached the maximum
303 depth in the early autumn. However, no significant relationship was detected between
304 DOC concentration and soil temperature at different depths. The DOC concentrations
305 in the upper organic soil layer increased considerably from early to late June, but did

306 not change significantly from July to late August. Across the entire growing seasons,
307 no significant relationship was found between the mean DOC concentration and the
308 mean soil temperature in the whole profile ($p > 0.05$, $n=4$).

309 The HIX, FI, and BIX of soil pore water varied greatly with soil depth (Fig. 8).
310 Pronounced changes in the three indices generally occurred at the depth where
311 organic soil transitioned to the mineral soil. HIX values gradually decreased with
312 depth while FI and BIX increased with depth. The fluorescence indices in the upper
313 organic soil layer changed significantly during the growing seasons. However, no
314 consistent from spring to autumn was found. The mean values for the three indices
315 were 16.62, 1.41, and 0.46 respectively in 2013. The data indicated a much higher
316 HIX level and a lower FI and BIX level in soil pore water than in the baseflow stream
317 discharge. HIX values were significantly and positively correlated to DOC
318 concentrations in soil pore water while FI and BIX were significantly but inversely
319 and correlated with DOC concentrations ($n = 18$, $p < 0.01$).

320

321 **Figure 7**

322

323 **Figure 8**

324

325 **4 Discussion**

326 **4.1 DOC concentrations and yield**

327 DOC concentrations in boreal rivers have been reported to vary considerably
328 according to differences in hydrology, soil type and topography (Andersson and
329 Nyberg, 2008; Tunaley et al., 2016; Broder et al., 2017). Theoretically, the presence
330 of organic soils in the catchment should contribute to higher DOC concentrations in
331 connected rivers. However, no direct relationship between organic soil content and
332 mean DOC concentration was extensively found across the boreal regions. In our

333 study, the annual mean concentration, 15.4 mg L^{-1} , was in the middle of the range of
334 concentrations reported from boreal regions, from 1.5 to 35.3 mg L^{-1} (Yates et al.,
335 2016; Avagyan et al., 2016). The DOC yield from our catchment was estimated at
336 $4.7 \text{ g m}^{-2} \text{ yr}^{-1}$, which was in the lower range of estimates reported for permafrost
337 region, which ranged from 1 to $35 \text{ g m}^{-1} \text{ yr}^{-1}$ (Fraser et al., 2001; Dinsmore et al.,
338 2010; Moody et al., 2016). The mean DOC yield in our catchment was less than the
339 net DOC loss reported from UK lands (2.1 - $11.5 \text{ g m}^{-2} \text{ yr}^{-1}$) (Moody et al., 2013), but
340 it was higher than in Finnish rivers ($3.5 \text{ g m}^{-2} \text{ yr}^{-1}$) (Räike et al., 2012), in the Yukon
341 River in Alaska (1.4 - $3.7 \text{ g m}^{-2} \text{ yr}^{-1}$) (Striegl et al., 2007), and in central Siberian
342 rivers (2.8 - $4.7 \text{ g m}^{-2} \text{ yr}^{-1}$) (Prokushkin et al., 2011). Pan Arctic rivers exported 32 Tg
343 C yr^{-1} of DOC to the Arctic Ocean according to estimates by Kichlighter et al. (2013),
344 which indicated a mean yield of $5.1 \text{ g m}^{-2} \text{ yr}^{-1}$ from the north Eurasian permafrost.
345 Our results indicated there was a slightly lower DOC yield in the southern part of the
346 Eurasian permafrost. However, our data are representative only of the region in
347 northeastern China. More field studies are needed to better estimate DOC loads from
348 the entire south Eurasia permafrost region.

349 Miao (2014) estimated the net ecosystem exchange (NEE) between peatland
350 surfaces and the atmosphere using both carbon dioxide and methane fluxes was
351 $30.59 \pm 1.98 \text{ g m}^{-2} \text{ yr}^{-1}$ in the study catchment. Therefore, the estimated DOC yield in
352 our study accounted roughly for 18.3% of the net ecosystem carbon balance in the
353 entire catchment. As the upland mountains, extensively covered by mineral soils,
354 likely export little DOC to the stream compared with the peatland, the actual DOC
355 yield based on the extent of the peatland will be much higher than $4.7 \text{ g m}^{-2} \text{ yr}^{-1}$.
356 Therefore, the yield generated by our study is a very conservative estimate. Even so,
357 our data still demonstrated the significant contribution of stream carbon export to the
358 net peatland ecosystem carbon balance. Any disturbance altering DOC export
359 processes and magnitudes will disrupt the balance between carbon sequestration and
360 release in the Eurasia peatlands. The proportion of stream carbon export in our study
361 was much higher than that in a northwest Russia river for which the DOC exported

362 by streamflow accounted for 5.6-8.5% of the total carbon sequestration in the
363 peatlands (Avagyan et al., 2016), but it was close to a peat catchment in Scotland, in
364 which DOC represented a loss of 24% of NEE (Dinsmore et al., 2010).

365 **4.2 Flow pathways, DOC sources and chemical characteristics**

366 Peatlands in permafrost regions generally experience subsurface flows but not
367 overland flows due to high rainfall infiltration into the thawed organic layer (Carey
368 and Woo, 1997). In our study, the porosity of peat in the upper 40 cm layer was
369 between 20-60%, which would necessarily allow rapid and high infiltration of rainfall.
370 The infiltrating rainfall was blocked from further vertical flow by the frozen soil, and
371 as a result flowed laterally towards the stream. Lateral subsurface flow was an
372 essential prerequisite for the positive relationship between discharge and the DOC
373 concentrations to avoid the dilution effect which would result from overland flow
374 (Guo et al., 2015).

375 The three fluorescence indices, HIX, FI, and BIX, exhibited considerable
376 fluctuations during rainfall-runoff events in our study, implying shifts in DOC sources
377 and chemical characteristics during subsurface flow. The three indices varied
378 vertically within the organic soil layer up to the mineral layer. Vertical trends were
379 maintained throughout the growing season of 2013 (Fig. 8). This pattern made the
380 indices good indicators of DOC sources. Given the significant correlation between the
381 indices and discharge, we concluded that the DOC released during flood periods
382 originated mostly from the upper organic soil layer, whereas the DOC during
383 recession and baseflow periods originated mainly from the lower mineral layer. Carey
384 and Woo (2001) described permafrost soil as a two-layer flow system based on the
385 difference in hydraulic conductivity between the upper organic soil and lower mineral
386 soil: Quickflow, defined as matrix flow or preferential flow in interconnecting soil
387 pipes and rills, took place in the highly porous peat in the upper layer, while slowflow
388 was laminar flow in the lower saturated mineral soils where flow velocities were
389 orders of magnitude lower than quickflow. As the porosity declined exponentially in
390 the transition from organic to mineral soil in the studied peatland, soil pore water in

391 the upper organic soil with high concentrations of DOC should be transported by
392 quickflow during floods, while baseflow conditions had much lower DOC
393 concentrations from the deeper mineral soil.

394 Seasonal shifts in DOC sources and composition have been reported in previous
395 studies in permafrost catchments (Spencer et al., 2008; O'Donnell et al., 2010).
396 However, our results highlighted the importance of the shifts temporally during runoff
397 event. In our study, the deepening of the soil active layer with thaw led to the
398 presence of vertical discontinuity in hydraulic conductivity in the discharge-yield
399 profile, and to shifts in DOC sources and chemical characteristics during runoff.
400 Because there were only a few rainfall events in 2014, we were able to identify the
401 effects of the gradual deepening of the active layer during the growing season as the
402 thawing proceeded. Significant increases in BIX and FI values during baseflow
403 occurred from the spring to the autumn in 2014 (Fig. 4). This implied a concomitant
404 increase in the proportion of microbial-derived DOC as the active layer deepened.
405 During thawing of the active layer, the hydraulic residence time and the DOC
406 mineralization rate, as well as physical adsorption in the mineral soil would increase
407 (Cronan and Aiken, 1985; Sebestyen et al., 2008), and this would alter DOC chemical
408 characteristics under baseflow conditions. The fact that DOC in soil pore water
409 exhibited higher HIX values and lower FI and BIX values compared to that in the
410 baseflow discharge was direct proof of adsorption-mineralization in the mineral soil
411 layer. DOC humification decreased and microbial-derived components increased
412 when DOC was delivered by slowflow across the mineral soil. Our result is consistent
413 with the study of Prokushkin et al. (2007) who also found higher levels of microbially
414 transformed and/or derived material export due to the presence of a deeper active
415 layer in the summer and autumn in Siberia. Changes in biochemical composition
416 (decreases in the lignocellulose complex; increases in the hydrophilic fraction) were
417 also confirmed by Kawahigashi et al. (2004). Based on these observations, a 9-11%
418 reduction in DOC load due to permafrost degradation was predicted in the Yukon
419 River by 2050 (Walvoord and Striegl, 2007), and an increase in dissolved inorganic

420 carbon was also hypothesized (Striegl et al., 2005). From these observations we infer
421 that deepening of the active layer in a warming climate conceivably could reduce
422 DOC export by baseflow, as well as alter DOC chemical characteristics to more
423 structure-simple microbial-derived components in the study region.

424 The HIX index for DOC showed no clear seasonal trend in the anomalously dry
425 year of 2014. Even a minor flood caused a large increase in HIX, implying the
426 sensitivity of DOC chemical characteristics to the shift in the primary flowpath from
427 quickflow to slowflow. The previous analysis had highlighted the importance of the
428 seasonal thawing of the active layer to flowpaths and DOC chemical characteristics.
429 Covariance analysis showed that the discharge quantity was the sole factor leading to
430 inter-annual variations in the DOC chemical characteristics. There was no significant
431 difference in the maximum thaw depths of the active layer for any of the three years
432 (Fig. 2), which was likely the reason why inter-annual effect of active layer thawing
433 could not be distinguished. In total, we conclude that there were different controlling
434 factors on DOC chemical characteristics depending on different temporal scales.
435 Long-term field investigations are crucially needed to evaluate in-depth the influence
436 of permafrost thaw on prevailing flowpaths and chemical characteristics of DOC.

437 **4.3 Discharge and DOC export**

438 We found a significant positive relationship between DOC concentration and
439 stream discharge, which is consistent with results observed in other permafrost
440 regions (Hinton et al., 1998; Petrone et al., 2007; Balcarczyk et al., 2009; Koch et al.,
441 2013). The positive relationship occurred in both the wet and the dry year, suggesting
442 that DOC export from the studied catchment is a transport-limited process.
443 Specifically, DOC transport capacity was mainly related to processes that controlled
444 runoff, for example flow path, rate of runoff and lag time. As described earlier, the
445 flowpath-shift was an equally important mechanism contributing to the positive
446 relationship between discharge and DOC concentrations. Our conclusion is supported
447 by both DOC model simulations (Neff and Asner, 2001; Wu, et al., 2014) and field
448 experiments (Tipping et al., 1999), reporting linear increases in DOC concentrations

449 with increasing amounts of subsurface flow.

450 It may be hypothesized that DOC is being generated in the peatland in amounts
451 large enough to make up for the loss of the DOC exported by successive floods in the
452 growing seasons. It is noteworthy that DOC concentrations were consistently high in
453 stream discharge during successive big floods in the autumn of 2012 and the spring of
454 2013. Meanwhile, the DOC concentrations in the organic soil layer of the peatland
455 remained at a stable high level about 40 mg L⁻¹ through the growing seasons.
456 Successive rainfalls and seasonal temperature variations did not result in decreased
457 concentrations in the peatland (Fig. 7). These data demonstrate the large DOC
458 productive potential of the peat soil.

459 The regression slopes for the positive relationships between DOC and discharge
460 showed large inter-annual variations (Fig. 4). The results of covariance analysis
461 indicated that were other factors besides discharge quantity underlay inter-annual
462 variations. The high sensitivity of DOC production and degradation to temperature
463 was well established (see Kalbitz et al., 2000; Moore et al., 2008). However, in our
464 study no significant relationships were found between the mean temperature and the
465 mean residual concentrations in the regression formulations for all three years (Table
466 3). Therefore temperature could not explain the residual variations. Precipitation also
467 was shown to be of great importance for DOC dynamics in boreal peatlands (for
468 example Olefeldt et al., 2013; Pumpanen et al., 2014). Discharge during flood events
469 can mobilize large quantities of pre-event water stored in the riparian zone (Kirchner,
470 2003; Winterdahl et al., 2011), and both the time interval of two successive rainfalls
471 and the quantity of the antecedent rainfall could influence DOC concentrations in the
472 second flood. It is possible that rainfall frequency during the growing seasons could
473 exert a cumulative effect on annual DOC dynamics. However, our data did not
474 provide conclusive evidence and more detailed and longer study is needed in this
475 regard. Nevertheless, the positive relationship between annual discharge and annual
476 mean DOC concentrations ($p < 0.05$, $n=3$) (Fig. 9) provided a simple tool to estimate
477 annual DOC load in the catchment.

478

479 **Figure 9**

480

481 **5 Conclusions**

482 Eurasian permafrost serves as an important potential carbon pool for the
483 atmosphere and for linked aquatic and ocean ecosystems. Investigations of DOC
484 responses in permafrost peatland could be used to predict the ecological consequences
485 of climatic change in these regions. Our study investigated the loads and determinants
486 of DOC export from a peatland catchment along the southern margins of Eurasian
487 permafrost. The catchment exhibited a relatively low DOC load compared to other
488 permafrost regions, and the yield estimates were an important contribution for
489 estimating global fluvial carbon export. DOC export in our study catchment was
490 transport-limited process as indicated by the positive correlation between discharge
491 and DOC concentrations in both wet and dry years. Field investigations indicated that
492 the source of the DOC and its chemical characteristics were greatly influenced by the
493 flowpath shifts between the upper organic soil layer and the lower mineral layer. The
494 shifts were closely related to the vertical soil structure and seasonal thawing of the
495 active layer. Deepening of active layer following permafrost degradation would
496 increase the content of microbial-originated DOC in baseflow discharge by increasing
497 the relative contribution from the lower mineral soil layer to the DOC pool. Our study
498 has provided limited field data on DOC dynamics in the southern region of Eurasian
499 permafrost. Additional more intensive studies are needed to improve our
500 understanding and predictions of the dynamics of DOC under future climate change.

501

502 **Acknowledgements**

503 The work was supported by National Key Research and Development Program of
504 China (2016YFA0602303), National Natural Science Foundation of China (41571097,

505 41730643), Key of Frontier Sciences, Chinese Academy of Sciences
506 (QYZDJ-SSW-DQC013), Research Program of Northeast Institute of Geography and
507 Agroecology, Chinese Academy of Science (IGA-135-05).

508

509 **References**

510 Ågren, A., Haei, M., Köhler, S. J., Bishop, K., and Laudon, H.: Regulation of stream
511 water dissolved organic carbon (DOC) concentrations during snowmelt; the role
512 of discharge, winter climate and memory effects, *Biogeosciences*, 7, 2901–2913,
513 2010.

514 Avagyan, A., Runkle, B. R. K., Hennings, N., Haupt, H., Virtanen, T., and Kutzbach,
515 L.: Dissolved organic matter dynamics during the spring snowmelt at a boreal river
516 valley mire complex in Northwest Russia, *Hydrol. Process.*, 30, 1727–1741, 2016.

517 Andersson, J-O. and Nyberg, L.: Spatial variation of wetlands and flux of dissolved
518 organic carbon in boreal headwater streams, *Hydrol. Process.*, 22, 1965–1975,
519 2008.

520 Balcarczyk, K.L., Jones Jr, J.B., Jaffé, R., and Maie, N.: Stream dissolved organic
521 matter bioavailability and composition in watersheds underlain with discontinuous
522 permafrost, *Biogeochemistry*, 94, 255–270, 2009.

523 Broder, T., Knorr, K. H., and Biester, H.: Changes in dissolved organic matter quality
524 in a peatland and forested headwater stream as a seasonality and hydrologic
525 conditions, *Hydrol. Earth Syst. Sci.*, 21, 2035–2051, 2017.

526 Carey, S. and Woo, M.K.: Snowmelt hydrology of two subarctic slopes, Southern
527 Yukon, Canada. In *Proceedings of the Eleventh Northern Research Basins
528 Symposium and Workshop (Vol 2)*, Prudhoe Bay/Fairbanks Alaska. The Water
529 and Environmental Research Centre, University of Alaska, Fairbanks, pp. 15–35,
530 1997.

531 Carey, S.K. and Woo, M.K.: Slope runoff processes and flow generation in a subarctic,

532 subalpine catchment, *J. Hydrol.*, 253, 110–129, 2001.

533 Cory, R.M., Ward, C.P., Crump, B.C., and Kling, G.W.: Sunlight controls water
534 column processing of carbon in arctic fresh waters, *Science*, 345, 925–928, 2014.

535 Cronan, C.S. and Aiken, G.R.: Chemistry and transport of soluble humic substances
536 in forested watersheds of the Adirondack Park, New York, *Geochim.
537 Cosmochim. Acta*, 49, 1697–1705, 1985.

538 Dinsmore, K.J., Billett, M.F., Skiba, U.M., Rees, R.M., Drewer, J., and Helfter, C.:
539 Role of the aquatic pathway in the carbon and greenhouse gas budgets of a
540 peatland catchment, *Global Change Biol.*, 16, 2750–2762, 2010.

541 Frey, K. E. and McClelland, J. W.: Impacts of permafrost degradation on arctic river
542 biogeochemistry, *Hydrol. Process.*, 23, 169–182, 2009.

543 Fraser, C.J.D., Roulet, N.T., and Moore, T.R.: Hydrology and dissolved organic
544 carbon biogeochemistry in an ombrotrophic bog, *Hydrol. Process.*, 15, 3151–3166,
545 2001.

546 Guo, Y.D., Song, C.C., Wan, Z.M., Tan, W.W., Lu, Y.Z., and Qiao, T.H.: Effects of
547 long-term land use change on dissolved carbon characteristics in the permafrost
548 streams of northeast China, *Environ. Sci.: Processes Impacts*, 16, 2496–2506, 16,
549 2014.

550 Guo, Y.D., Song, C.C., Wan, Z.M., Lu, Y.Z., Qiao, T.H., Tan, W.W., and Wang, L.L.:
551 Dynamics of dissolved organic carbon release from a permafrost wetland
552 catchment in northeast China. *J. Hydrol.*, 531, 919–928, 2015.

553 Hinton, M.J., Schiff, S.L., and English, M.C.: Sources and flowpaths of dissolved
554 organic carbon during storms in two forested watersheds of the Precambrian
555 Shield. *Biogeochemistry*, 41, 175–197, 1998. doi:10.1023/A:1005903428956

556 Huguet, A., Vacher, L., Relexans, S., Saubusse, S., Froidefond, J.M., and Parlanti, E.:
557 Properties of fluorescent dissolved organic matter in the Gironde Estuary, *Org.
558 Geochem.*, 40, 706–719, 2009.

559 Jin, H.J., Li, S.X., Cheng, G.D., Wang, S.L., and Li, X.: Permafrost and climatic
560 change in China, *Global Planet., Change* 26, 387–404, 2000.

561 Kalbitz, K., Soliiger, S., Park, J.H., Michalzik, B., and Matzner, E.: Controls on the
562 dynamics of dissolved organic matter in soils: A review, *Soil Sci.*, 165, 277–304,
563 2000.

564 Kalbitz, K., Schwesig, D., Rethemeyer, J., and Matzner, E.: Stabilization of dissolved
565 organic matter by sorption to the mineral soil, *Soil Biol Biochem.*, 37, 1319–1331,
566 2005.

567 Kawahigashi, M., Kaiser, K., Kalbitz, K., Rodionov, A., and Guggenberger, G.:
568 Dissolved organic matter in small streams along a gradient from discontinuous to
569 continuous permafrost, *Global Change Biol.*, 10, 1576–1586, 2004.

570 Kicklighter, D. W., Hayes, D. J., McClelland, J. W., Peterson, B. J., McGuire, A. D.,
571 and Melillo, J. M.: Insights and issues with simulating terrestrial DOC loading of
572 Arctic river networks, *Ecol. Appl.*, 23, 1817–1836, 2013.

573 Kirchner, J.W.: A double paradox in catchment hydrology and geochemistry, *Hydrol.*
574 *Processes*, 17, 871–874, 2003.

575 Koch, J.C., Runkel, R.L., Striegl, R., and McKnight, D.M.: Hydrologic controls on
576 the transport and cycling of carbon and nitrogen in a boreal catchment underlain by
577 continuous permafrost, *J. Geophys. Res-Biogeo.*, 118, 698–712, 2013.
578 doi:10.1002/jgrg.20058,

579 Laudon, H., Berggren, M., Ågren, A., Buffam, I., Bishop, K., Grabs, T., Jansson, M.,
580 and Köhler, S.: Patterns and dynamics of dissolved organic carbon (DOC) in
581 boreal streams: the role of processes, connectivity, and scaling, *Ecosystems*, 14,
582 880–893, 2011.

583 Lessels, J.S., Tetzlaff, D., Carey, S.K., Smith, P., and Soulsby, C.: A coupled
584 hydrology-biogeochemistry model to simulate dissolved carbon exports from a
585 permafrost-influenced catchment. *Hydro. Process.*, 29, 5383–5396, 2015.

586 Lyon, S. W., Destouni, G., Giesler, R., Humborg, C., Mörth, M., Seibert, J., Karlsson,
587 J., and Troch, P. A.: Estimation of permafrost thawing rates in a sub-arctic
588 catchment using recession flow analysis, *Hydrol. Earth Syst. Sci.*, 13, 595–604,
589 2009.

590 Lyon, S.W., Morth, M., Humborg, C., Giesler, R., and Destouni, G.: The relationship
591 between subsurface hydrology and dissolved carbon fluxes for a sub-arctic
592 catchment, *Hydrol. Earth Syst. SC.*, 14, 941–950, 2010.

593 Mann, P.J., Davydova, A., Zimov. N., Spence, R.G.M., Davydov, S., Bulygina, E.,
594 Zimov, S., and Holmes, R.M.: Controls on the composition and liability of
595 dissolved organic matter in Siberia’s Kolyma river basin, *J. Geophys. Res-Bioge.*,
596 117, G01028, doi: 10.1029/2011JG001798, 2012.

597 McKnight, D. M., Boyer, E. W., Westerhoff, P. K., Doran, P. T., Kulbe, T., and
598 Andersen, D. T.: Spectrofluorometric characterization of dissolved organic matter
599 for indication of precursor organic material and aromaticity, *Limnol. Oceanogr.*,
600 46, 38–48, 2001.

601 Miao, Y.Q.: Net ecosystem carbon fluxes of peatland in the continuous permafrost
602 zone, Great Hinggan Mountains. Dissertation. University of Chinese Academy of
603 Sciences. pp, 120, 2014. (in Chinese)

604 Moody, C.S., Worrall, F., and Burt, T.P.: Identifying DOC gains and losses during a
605 20-year record in the Trout Beck catchment, Moor House, UK, *Ecol. Indic.*, 68,
606 102–114, 2016.

607 Moody, C.S., Worrall, F., Evas, C.D., and Jones, T.G.: The rate of loss of dissolved
608 organic carbon (DOC) through a catchment, *J. Hydrol.*, 492, 139–150, 2013.

609 Moore, T. R., Paré, D., and Boutin R.: Production of dissolved organic carbon in
610 Canadian forest soils, *Ecosystems*, 11, 740–751, 2008.

611 Neff, J. C. and Asner, G. P.: Dissolved organic carbon in terrestrial ecosystems:
612 synthesis and a model, *Ecosystems*, 4, 29–48, 2001.

613 Ohno, T.: Fluorescence inner-filtering correction for determining the humification
614 index of dissolved organic matter, *Environ. Sci. Technol.*, 36, 742–746, 2002.

615 O’Donnell, J. A., Aiken, G. R., Kane, E. S., and Jones, J. B.: Source water controls on
616 the character and origin of dissolved organic matter in streams of the Yukon River
617 basin, Alaska, *J. Geophys. Res.*, 115, G03025, doi:10.1029/2009JG001153, 2010.

618 Olefeldt, D., Roulet, N., Giesler, R., and Persson, A.: Total waterborne carbon export
619 and DOC composition from ten nested subarctic peatland catchments-importance
620 of peatland cover, groundwater influence, and inter-annual variability of
621 precipitation patterns. *Hydrol. Process.*, 27, 2280–2294, 2013.

622 Opsahl, S., Benner R., and Amon R. M. W.: Major flux of terrigenous dissolved
623 organic matter through the Arctic Ocean, *Limnol. Oceanogr.*, 44, 2017–2023,
624 1999.

625 Park, Y.S., Engel, B.A., Frankenberger, J., and Hwang, H.: A-web-based tool to
626 estimate pollutant loading using LOADEST, *Water*, 7, 4858–4868, 2015.

627 Petrone, K.C., Jones, J.B., Hinzman, L.D., and Boone, R.D.: Seasonal export of
628 carbon, nitrogen, and major solutes from Alaskan catchments with discontinuous
629 permafrost, *J. Geophys. Res.*, 111, G02020, doi:10.1029/2005JG000055, 2006.

630 Petrone, K.C., Hinzman, L.D., Shibata, H., Jones, J.B., and Boone, R.: The influence
631 of fire and permafrost on sub-arctic stream chemistry during storms, *Hydrol.*
632 *Process.*, 21, 423–434, 2007.

633 Prokushkin, A.S., Pokrovsky, O. S., Shirokova, L.S., Korets, M.A., Viers, J.,
634 Prokushkin, S.G., Amon, R. M. W., Guggenberger, G., and McDowell, W.H.:
635 Sources and the flux pattern of dissolved carbon in rivers of the Yenisey basin
636 draining the Central Siberian Plateau, *Environ. Res. Lett.*, 6, 045212,
637 doi:10.1088/1748-9326/6/4/045212, 2011.

638 Prokushkin, A.S., Gleixner, G., McDowell, W.H., Ruehlow, S., and Schulze, E.D.:
639 Source and substrate-specific export of dissolved organic matter from
640 permafrost-dominated forested watershed in central Siberia, *Global Biogeochem.*

641 Cy., 103, 109–124, 2007.

642 Pumpanen, J., Linden, A., Miettinen, H., Kolari, P., Ilvesniemi, H., Mammarella,
643 I., Hari, P., Nikinmaa, E., Heinonsalo, J., Back, J., Ojala, A., Berninger, F., and
644 Vesala, T.: Precipitation and net ecosystem exchange are the most important
645 drivers of DOC flux in upland boreal catchments, *J. Geophys. Res.-Biogeo.* 119,
646 1861–1878, 2014.

647 Räike, A., Kortelainen, P., Mattsson, T., David N., and Thomas, D. N.: 36 year trends
648 in dissolved organic carbon export from Finnish rivers to the Baltic Sea, *Sci. Total*
649 *Environ.*, 435–436, 188–201, 2012.

650 Sebestyen, S.D., Boyer, E.W., Shanley, J.B., Kendall, C., Doctor, D.H., Aiken, G.R.,
651 and Ohte, N.: Sources, transformations and hydrological processes that control
652 stream nitrate and dissolved organic matter concentrations during snowmelt in an
653 upland forest, *Water Resour. Res.*, 44, W12410, doi:10.1029/2008WR006983,
654 2008.

655 Spencer, R. G. M., Aiken, G. R., Wickland, K. P., Striegl, R. G., and Hernes, P. J.:
656 Seasonal and spatial variability in dissolved organic matter quantity and
657 composition from the Yukon River basin, Alaska, *Global Biogeochem. Cycles*, 22,
658 GB4002, doi:10.1029/2008GB003231, 2008.

659 Spencer, R.G., Mann, P.J., Dittmar, T., Eglinton, T.I., McIntyre, C., Holmes, R.M.,
660 Zimov, N., and Stubbins, A.: Detecting the signature of permafrost thaw in Arctic
661 rivers, *Geophys. Res. Lett.*, 42(8), 2830–2835, 2015.

662 Striegl, R. G., Aiken, G. R., Dornblaser, M. M., Raymond, P. A., and Wickland, K. P.:
663 A decrease in discharge-normalized DOC export by the Yukon River during
664 summer through autumn, *Geophys. Res. Lett.*, 32, L21413,
665 doi:10.1029/2005GL024413, 2005.

666 Striegl, R. G., Dornblaser, M. M., Aiken, G. R., Wickland, K. P., and Raymond, P. A.:
667 Carbon export and cycling by the Yukon, Tanana, and Porcupine rivers, Alaska
668 2001–2005, *Water Resour. Res.*, 43, W02411, doi:10.1029/2006WR00, 2007.

669 Tipping, E., Woof, C., Rigg, E., Harrison, A. F., Inneson, P., Taylor, K., Benham, D.,
670 Poskitt, J., Rowland, A. P., Bol, R., and Harkness, D. D.: Climatic influences on the
671 leaching of dissolved organic matter from upland UK moorland soils, investigated
672 by a field manipulation experiment, *Environ. Inter.*, 25, 83–95, 1999.

673 Townsend-Small, A., McClelland, J. W., Max Holmes, R., and Peterson, B. J.:
674 Seasonal and hydrologic drivers of dissolved organic matter and nutrients in the
675 upper Kuparuk River, Alaskan Arctic, *Biogeochemistry*, 103,109–124, 2011.

676 Tunaley, C., Tetzlaff, D., Lessels, J., and Soulsby, C.: Linking highfrequency DOC
677 dynamics to the age of connected water sources, *Water Resour. Res.*, 52, 5232–
678 5247, 2016.

679 Vonk, J.E., Mann, P.J., Davydov, S., Davydova, A., Spencer, R.G.M., Schade, J.,
680 Sobczak, W.V., Zimov, N., Zimov, S., Bulygina, E., and Eglinton, T.I.: High
681 biolability of ancient permafrost carbon upon thaw, *Geophys. Res. Lett.*, 40,
682 2689–2693, 2013.

683 Walvoord, M. A. and Striegl, R. G.: Increased groundwater to stream discharge from
684 permafrost thawing in the Yukon River basin: Potential impacts on lateral export
685 of carbon and nitrogen, *Geophys. Res. Lett.*, 34, L12402,
686 doi:10.1029/2007GL030216, 2007.

687 Winterdahl, M., Futter, M., Köhler, S., Laudon, H., Seibert, J., and Kevin, B.K.:
688 Riparian soil temperature modification of the relationship between flow and
689 dissolved organic carbon concentration in a boreal stream. *Water Resour. Res.*, 47,
690 W08532, doi:10.1029/2010WR010235, 2011.

691 Wu, H., Peng, C., Moore, T.R., Hua, D., Li, C., Zhu, Q., Peichl, M., Arain, M.A., and
692 Guo, Z.: Modeling dissolved organic carbon in temperate forest soils:
693 TRIPLEX-DOC model development and validation, *Geosci. Model Dev.*, 7, 867–
694 881, 2014.

695 Yates, C.A., Johnes, P.J., and Spencer, R. G. M.: Assessing the drivers of dissolved
696 organic matter export from two contrasting lowland catchments, U.K, *Sci. Total*

697 Environ., 569–570, 1330–1340, 2016.

698

699

700

701

702

703 **Table 1.** Mean annual DOC loads, concentrations and yields estimated by LOADEST

704 program for 2012-2014.

Period	Load (kg)			Concentration (mg L ⁻¹)			Yield (g m ⁻²)		
	SE			CV (%)			SE		
	2012	2013	2014	2012	2013	2014	2012	2013	2014
May	1388	66502	4238	9.00	35.49	15.04	0.08	6.02	0.40
	<i>161</i>	<i>7479</i>	<i>194</i>	<i>39.3</i>	<i>25.2</i>	<i>30.5</i>	<i>0.009</i>	<i>0.13</i>	<i>0.06</i>
June	5917	3728	3574	16.53	17.92	15.88	0.62	0.39	0.37
	<i>619</i>	<i>235</i>	<i>164</i>	<i>30.4</i>	<i>26.0</i>	<i>16.4</i>	<i>0.02</i>	<i>0.07</i>	<i>0.07</i>
July	3372	12228	4056	14.08	16.76	15.02	0.36	1.32	0.44
	<i>268</i>	<i>1261</i>	<i>191</i>	<i>26.9</i>	<i>19.6</i>	<i>24.0</i>	<i>0.09</i>	<i>0.04</i>	<i>0.07</i>
August	9385	14475	2194	13.35	16.14	11.32	1.01	1.56	0.24
	<i>982</i>	<i>1394</i>	<i>95</i>	<i>48.1</i>	<i>49.8</i>	<i>12.7</i>	<i>0.03</i>	<i>0.15</i>	<i>0.03</i>
September	8788	3875	1977	11.12	13.49	10.09	0.77	0.38	0.19
	<i>870</i>	<i>471</i>	<i>106</i>	<i>48.3</i>	<i>26.7</i>	<i>11.3</i>	<i>0.03</i>	<i>0.03</i>	<i>0.03</i>
Annual	6092	19022	3211	13.26	19.57	13.48	2.84	9.68	1.64
	<i>423</i>	<i>1521</i>	<i>89</i>	<i>38.6</i>	<i>29.4</i>	<i>19.0</i>	<i>0.18</i>	<i>0.38</i>	<i>0.26</i>

705

706

707

708

709

710

711

712

713

714

715

716

717

718 **Table 2** Results of covariance analysis (ANCOVA) between discharge and the DOC
719 concentrations for the 2012-2014 sampling periods.

Source	Sum of squares	df	Mean squares	F.	Sig.
Corrected model	2895.334	3	965.111	41.213	0.000
Log ₁₀ Q	2026.994	1	2026.994	86.559	0.000
Year	303.294	2	151.647	6.476	0.002
Error	2294.932	98	23.418		

720 DOC concentrations and log₁₀Q are dependent variable and covariate respectively;
721 Year denotes fixed factor; Adjusted mean annual concentrations for the three years are
722 15.25±0.88, 18.32±0.84, and 14.22±0.81 mg L⁻¹ in turn.

723

724

725 **Table 3.** Results of linear regression analysis between discharge and the DOC
726 concentrations for the 2012-2014 sampling periods.

Model	2012			2013			2014		
	DF	Sum of Squares	Mean Square	DF	Sum of Squares	Mean Square	DF	Sum of Squares	Mean Square
Regression	1	690.85	690.85	1	1582.96	1582.96	1	271.18	271.18
Residual	34	558.21	16.45	33	1032.80	31.30	29	185.92	6.41
Total	35	1249.06		34	2615.76		30	457.10	

727

728

729

730

731

732

733 **Table 4.** Correlation analysis of the three fluorescence indices with hydrological and
 734 climatic factors.

		DOC	Q	Conductivity	Turbidity	T _{air}	T _{soil}
HIX	Pearson	0.708**	0.609*	0.451**	-0.592**	0.342	0.395*
	Sig. (2-tailed)	0.000	0.000	0.005	0.000	0.115	0.02
	n	92	92	68	68	92	92
FI	Pearson	-0.594**	-0.606**	-0.477**	0.469**	0.353	0.389
	Sig. (2-tailed)	0.000	0.000	0.004	0.001	0.203	0.128
	n	92	92	68	68	92	92
BIX	Pearson	-0.64**	-0.707**	-0.488**	0.322*	-0.027	0.384
	Sig. (2-tailed)	0.001	0.000	0.001	0.012	0.823	0.129
	n	92	92	68	68	92	92

735 DOC is dissolved organic carbon; Q is stream discharge; T_{air} is the average air
 736 temperature over the past three days; T_{soil} is the average soil temperature of the active
 737 layer; “***” denotes p < 0.01; “*” denotes p < 0.05

738

739

740

741

742 **Table 5.** Results of covariance analysis (ANCOVA) between discharge and the
743 fluorescence indices for the study period.

Index	Source	Sum of squares	df	F.	Sig.
HIX	Log ₁₀ Q	296.045	1	70.315	0.000
	Year	9.318	2	1.107	0.335
FI	Log ₁₀ Q	0.097	1	63.490	0.000
	Year	0.007	2	2.128	0.125
BIX	Log ₁₀ Q	0.084	1	86.098	0.000
	Year	0.004	2	1.850	0.163

744

745 The indices, HIX, FI, and BIX, are set as dependent variables; log₁₀Q is covariate; Year
746 denotes fixed factor.

747

748

749

750

751

752

753

754

|

755
756
757
758
759
760
761
762
763
764
765
766
767
768
769
770
771
772
773
774
775
776
777
778
779
780
781
782
783
784
785
786
787
788
789
790
791
792
793
794

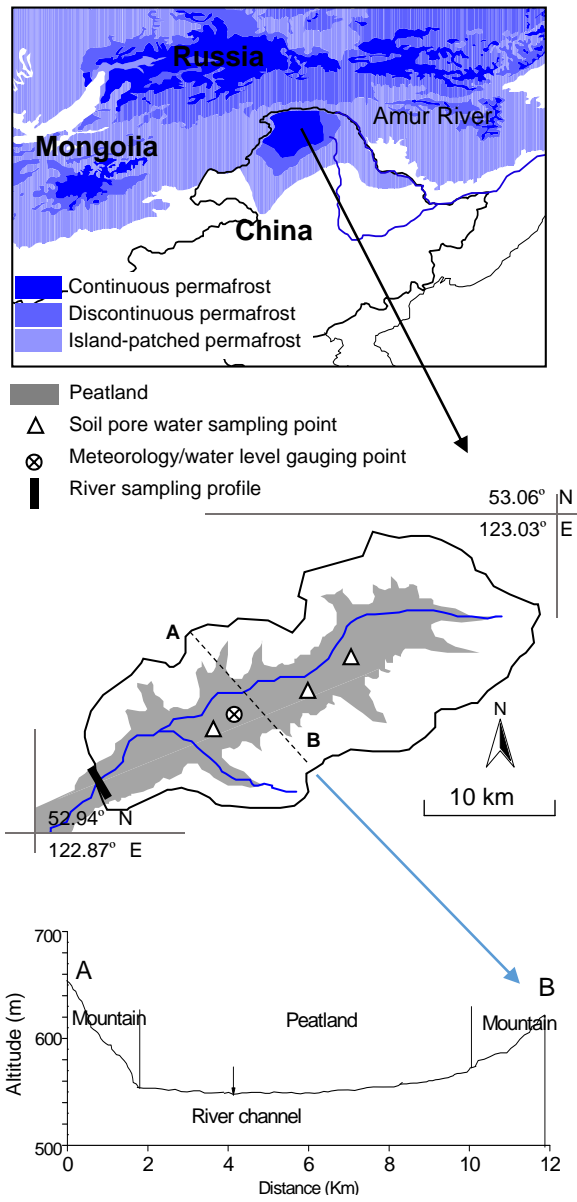


Figure 1: Geographic location of the study area

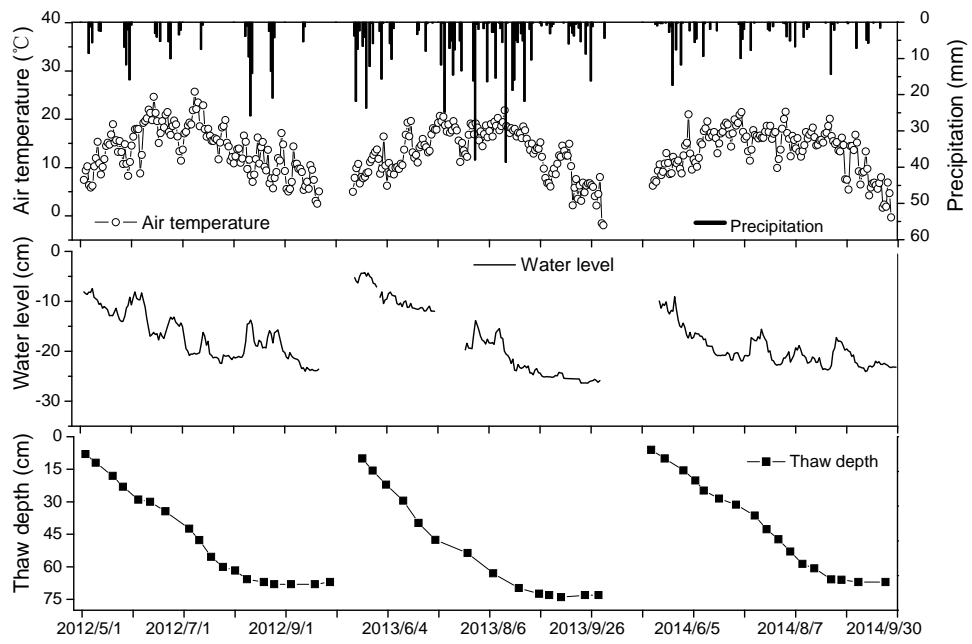


Figure 2: Air temperature, precipitation, water levels in peatland, and thaw depth observed during the growing seasons of 2012 to 2014.

813

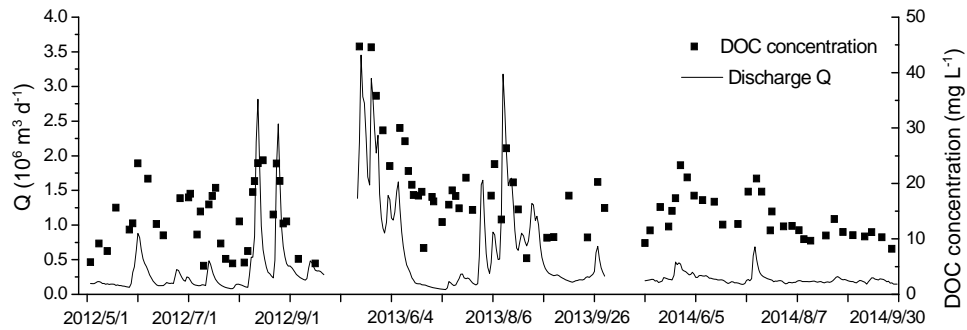
814

815

816

817

818



819 **Figure 3: Dissolved organic carbon (DOC) concentrations and discharge (Q) observed**

820 **during the growing seasons of 2012 to 2014.**

821

822

823

824

825

826

827

828

829

830

831

832

833

834

835

836
837
838
839
840
841
842
843
844
845
846
847
848
849
850
851
852
853
854
855
856
857
858
859
860
861
862

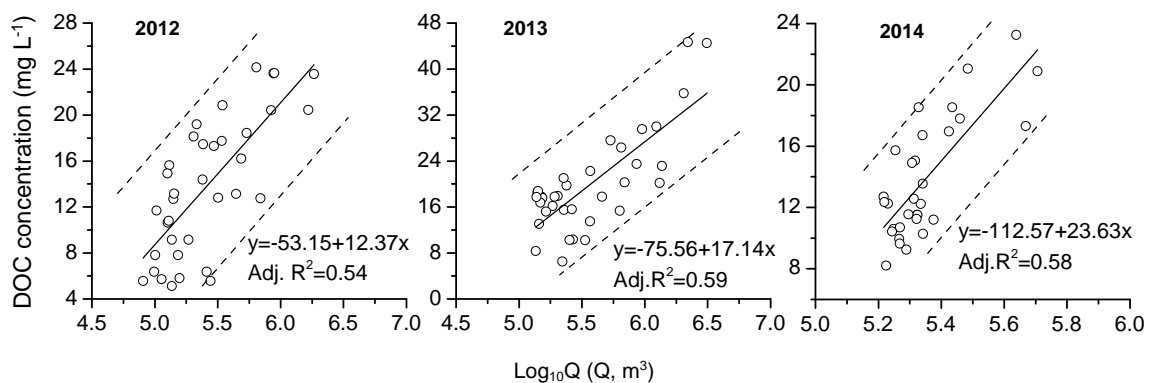


Figure 4: Relationships between discharge (Q) and the DOC concentrations for 2012-2014 sampling periods.

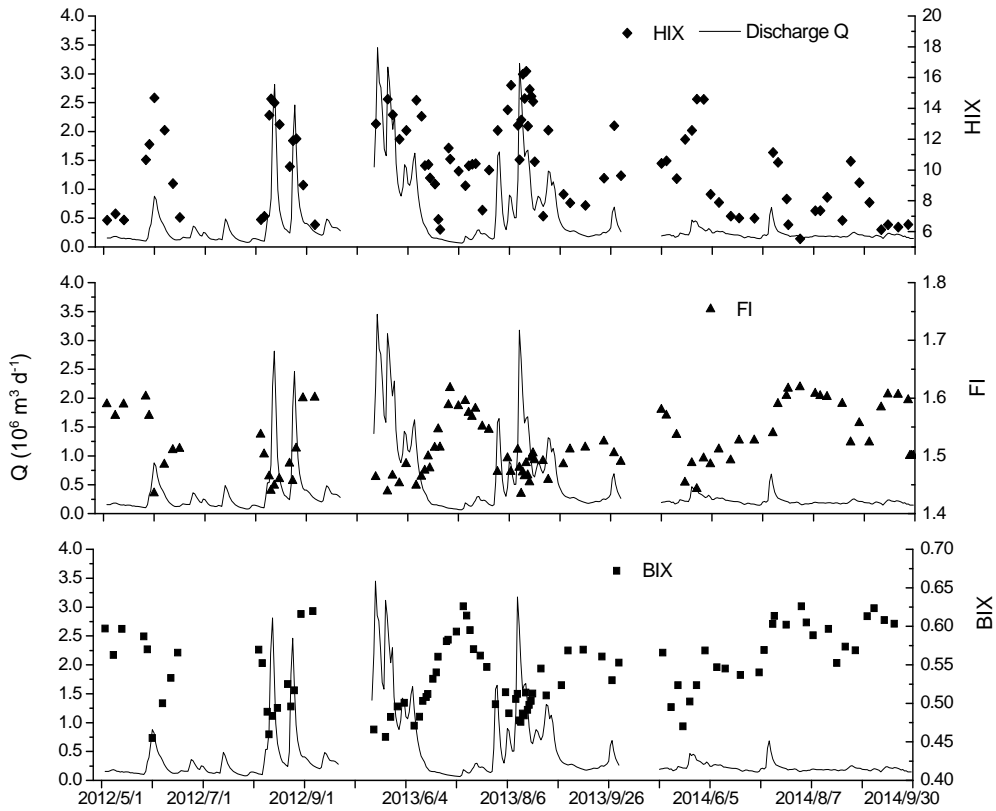
863

864

865

866

867



873

874 **Figure 5: Dynamics of the three spectral indices following discharge (Q) during the 2012-**

875 **2014 sampling period.**

876

877

878

879

880

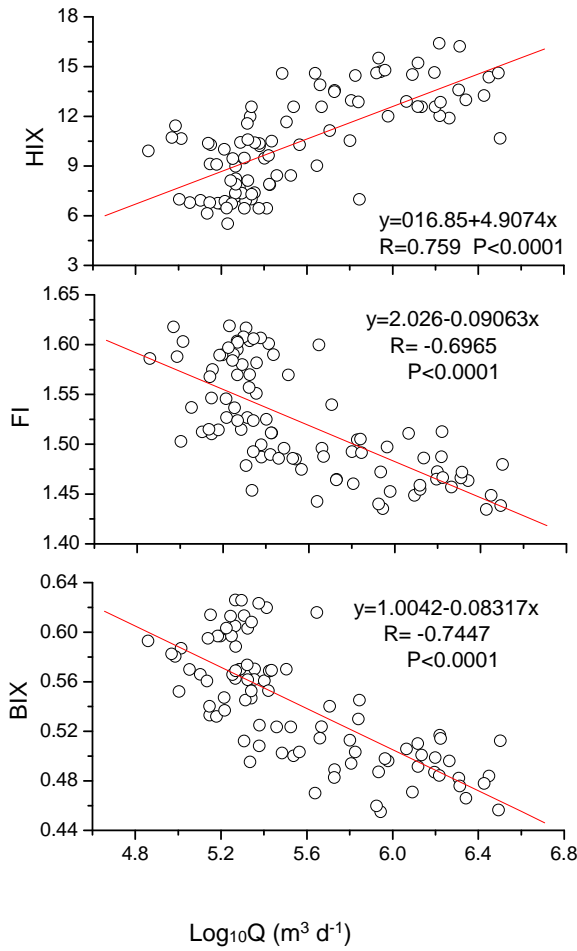
881

882

883

884

885



886

887

888

889

890

891

892

893 **Figure 6: Relationships between discharge (Q) and the three indices during the 2012-2014**

894 **sampling period.**

895

896

897

898

899

900

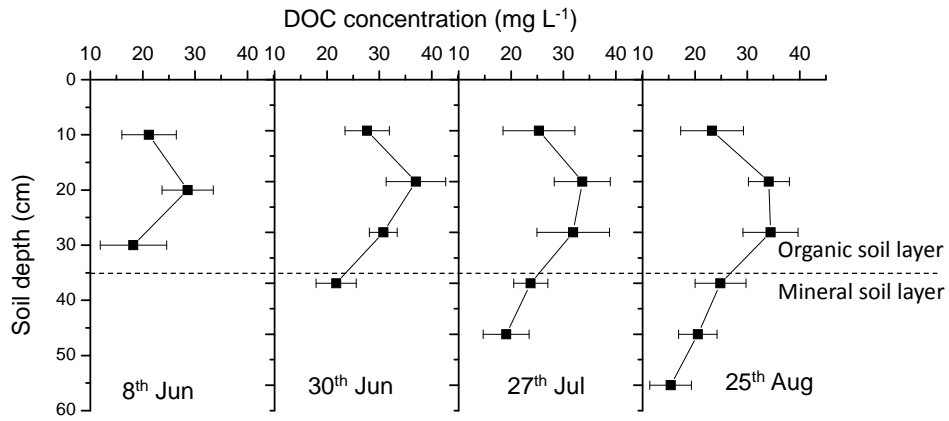
901

902

903

904

905



906

Figure 7: DOC concentrations in soil pore water along the soil profile in 2013.

907

908

909

910

911

912

913

914

915

916

917

918

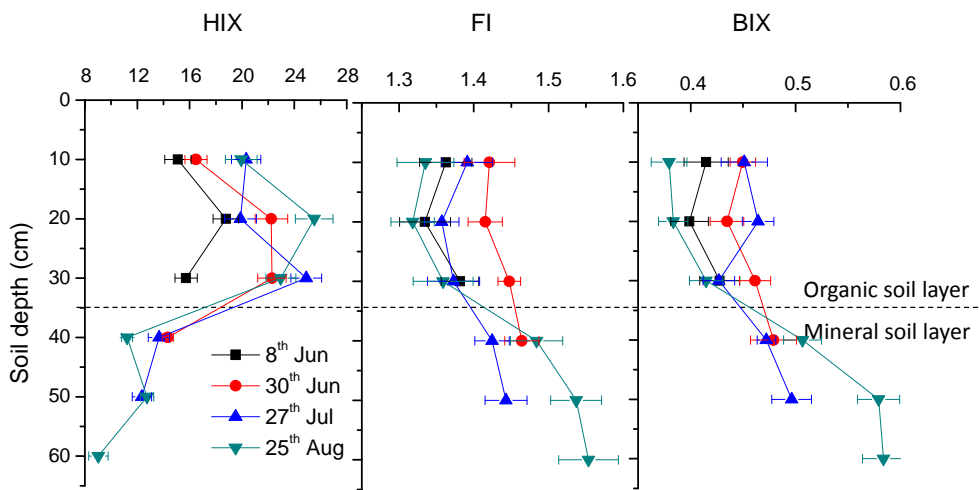
919

920

921

922

923



924 **Figure 8: Vertical distribution of the three spectral indices for soil pore water along the soil**

925 **profile in 2013.**

926

927

928

929

930

931

932

933

934

935

936

937

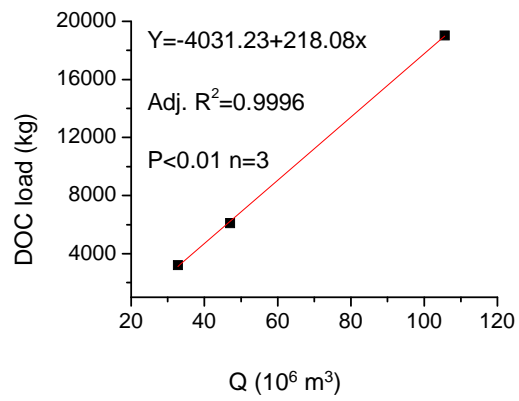
938

939

940

941

942



943 **Figure 9: Relationship between annual discharge (Q) and DOC load for the three years.**